

Modelling on Reinforced Concrete Exterior Joint with Simplified Detailing Technique by Using Coupler Bar

Marimuthu. K, Kothandaraman. S

Abstract: *The present study focus on structural response of the Reinforced Concrete (RC) beam-column joint through numerical studies. For this study, totally two groups of reinforcement details are considered and named as "EJ-SFC" and "EJ-IS456". The proposed coupler joint specimen (EJ-SFC) is compared with the standard detailed specimen that is design and detailed by IS 456-2000. To simulate each group of the specimen, a full 3D Finite Element Modelling (FEM) analysis has been carried out by using ANSYS 14.5 software. All groups of joints were tested under reverse cyclic loading. The outcome of the Finite Element Analysis (FEA) findings were presented in terms of load - deflection plot and compared with previous experimental results. The FEA and experimental results showed that the performance of the proposed coupler joint specimen was superior in ductile behaviour than that of EJ-IS456 specimen.*

Index Terms: *Reinforced concrete, Beam-column joint, Flat coupler bar, Reverse cyclic loading, Finite element method.*

I. INTRODUCTION

In a reinforced concrete structure, the beam-column joint is the weakest element against seismic loading than that of slab, column and beam. It requires proper design and detailing and these are playing a key role in providing sufficient strength and ductility. The strength and ductility can be achieved by providing a sufficient amount of hoop reinforcement and sufficient anchorage length to the beam main bar. A huge amount of research has been carried out to improve the existing detailing/technique by experimentally and numerically. To improve the anchorage behavior, Kotsova and Mouzakis (2011) have used a steel plate technique to anchor the beam main longitudinal bar. In this technique, a steel plate has been attached at the end of the beam main bar at core joint and all the main bars have threaded at their ends and connected by nuts. From the experimental results, they have concluded that the use of this technique with an inclined bar arrangement in the core region exhibits superior behaviour, reduce number of stirrups and steel congestion. Karayannis (2014) has investigated the effect of spiral reinforcement in RC exterior joint through both experimentally and theoretically. The results of the study showed superior behaviour in terms of ultimate load and load-displacement behaviour than that of control specimen. Muhsen and

Umemura (2011) collected the details of joints from previous research work and created a new database. On the basis of the new database, they have developed a new model for calculating the shear strength of the joint. The proposed new model showed improved performance in calculating the shear strength of the joint. Kang (2012) developed the binomial logistic regression methodology from an experimental database to determine the behaviour of the joint and he found that the effective achievement of the joint in behaviour depends on head size, head thickness and development of the bar. The performance of the joint was increased by increasing the geometry of head size and development length of the bar. Also, they determined that the most influencing joint parameters were joint shear demand and bar yield stress. Tran (2016) investigated the parameters affecting the shear strength of the joint. For constructing a database, 172 RC beam-column connections (experimental) were taken. From the study, they have found that vertical and horizontal joint hoops, compressive strength of concrete, beam bar detail index and column axial stress are affecting the joint shear strength. Kim and LaFave (2007) have reported that the compressive strength is one of the most influencing parameter for joint shear strength. Ronagh and Baji (2017) presented the load-displacement behaviour of FRP strengthened RC beam-column joint through Ansys and VecTor2 program. From their study, they have concluded that the performance of both the programs was excellent in cyclic loading condition and the performance of VecTor2 programme in the case of seismic type of loading was excellent than that of Ansys. Also, both the programs were very efficient to predict strength, yield displacement and crack behaviour. Sagbas et al (2011) carried out an analytical investigation to find the effectiveness of FEM procedure in capturing the behaviour of beam-column joints. Totally 12 test specimens were used and a model was created by using VecTor2. From the computed results, they concluded that the non-linear FE analysis procedure could be an accurate and reliable tool for determining the behavior of both

Revised Manuscript Received on July 09, 2019

Marimuthu. K., Research Scholar, Department of Civil Engineering, Pondicherry Engineering College, Puducherry.

Kothandaraman. S., Professor, Department of Civil Engineering, Pondicherry Engineering College, Puducherry

seismic and non-seismic designed beam-column joint. By using this tool, accurate simulation can be achieved. Li and Tran (2009) experimentally and numerically investigated the effect of vertically distributed longitudinal reinforcement layer in the beam. Four full-scale test specimens were tested under quasi-static cyclic loading. The experimental results were compared with FEM results in terms of hysteresis loops, failure mechanism and crack pattern. The experimental results showed that improved behaviour was observed in strength and energy absorption capacity and these experimental results were matched with FEA results. Hatch (2007) reported the influence of axial load on the exterior joint specimen through numerical studies by using the software ABAQUS. The results of the experiment indicated that the column axial load introduced tension stress in beam main bar and made the joint very stiff. Hegger (2004) studied the behaviour and factors affecting the shear strength of the joint numerically by creating a model for the joint using the nonlinear FEM program ATENA. He found that a very good agreement was observed between experimental and numerical studies by comparing the FE results with the proposed theoretical equation as well as experimental. From the above literature study, it is found that the seismic joint requires higher percentage of stirrups for both column and beam element. The national and international codes are strongly recommended the above requirement. The use of higher amount of transverse reinforcement in the joint cause serious congestion and construction problem and these leads to reduction in the strength as well as rapid deterioration in the joint region. To overcome the above difficulty, a new reinforcing technique has been introduced in the core region of the joint. In this technique, a steel flat coupler has been introduced at the core of the joint for anchoring the beam main bar. The use of new reinforcing technique exhibits a very good anchorage for beam main bar, less congestion, easy installation, higher ductility and less deterioration. To prove the efficiency of the proposed reinforcement technique, Finite Element Analysis (FEA) study was performed with the help of ANSYS 14.5 software. The FEA results showed that the proposed technique is performed better than that of conventional joint in terms of strength and ductility. From the ductility point of view, the proposed joint was performed excellent and it can be used as an alternate option for conventional reinforcing technique.

II. RESEARCH SIGNIFICANT

The seismic beam-column joint required standard ninety-degree hook with large development length for anchoring beam main bar in the core of the joint region which leads to serious steel congestion and creates many construction issues during the execution of work. The beam-column joint is a confined region. Handling and placing the main bar in this smaller region is very difficult. It requires more time and labour. The use of steel flat coupler bar in the core region offers a possible solution for the above mentioned problems and use of this technique in the core region exhibits improved behaviour in terms of strength, ductility and hysteresis behaviour.

III. DETAILS OF SPECIMEN

Two categories of half-scaled exterior joint were chosen for FEA study. The designation of the exterior joint specimen is EJ-SFC and EJ-IS456. The first group of specimen named as control specimen (EJ-SFC) and reinforcement detailing including anchorage device is illustrated in Fig. 1. Similarly, the second group of specimen (EJ-IS456) was used as a comparative specimen and detailing for this category is illustrated in Fig. 2. In the second group of the specimens (EJ-IS456), the confinement (shear reinforcement) and anchorage for beam main bar details were provided as per IS456-2000. For all the categories, the geometry and configuration were common and the Fig. 1 and Fig. 2 shows the size of the column and beam. For all the categories, the concrete grade (M20) and steel grade (Fe500) were same. The size of the column was 175x125mm and height of the column was 1500mm. The column main bar was reinforced with 4 numbers of 10mm diameter bar and 6mm diameter bar was used as shear reinforcement. Similarly, the cross section of the beam was 125x175mm and length of the beam was 900mm. The beam main bar was reinforced with 4 numbers of 10mm diameter bar and 6mm diameter bar was used as stirrups reinforcement. The spacing of the ties for the column was 125mm c/c and the beam was 110 mm c/c. For both the group of the specimens, the column and the beam main bar were same; that is 10mm diameter. Similarly, the shear reinforcement for both the groups of specimens was same; that is 6mm diameter. The spacing of the shear reinforcement for both the columns were 6mm dia 125mm c/c and the beam were 6mm diameter 110mm c/c. In the proposed joint, the main reinforcement was anchored by steel flat coupler which is shown in Fig. 1. For the second group of specimens, the beam main bar was anchored by standard ninety-degree hook as per IS456-2000 code requirement. The loading and boundary condition were same for both the groups of the specimens. A constant axial of 40kN was given at the column top and the cyclic load was given at the tip of the beam. The test was performed under reverse cyclic loading condition and results were presented in terms of load-deflection graph.

IV. NUMERICAL METHOD (FEM)

A. Element type used

For modelling the concrete element, linear isotropic element Solid65 was used. These elements have capacity for deformation, crushing in compression and cracking in tension. Solid65 elements have eight nodes and each node having three degrees of freedom. For defining the material, the value of EX (Young's modulus) and PRXY (Poisson's ratio) were taken as 30.8 N/mm² and 0.16 respectively. The co-efficient of the shear transfer is 0.3 for open crack and 0.9 for closed crack.



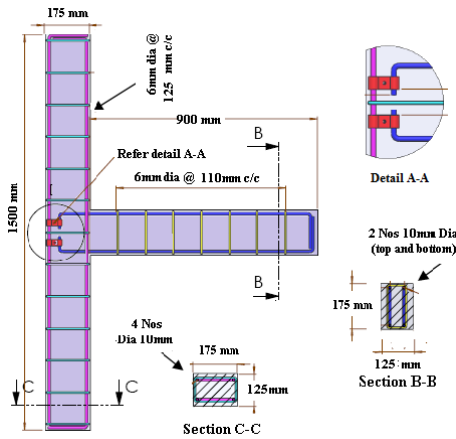


Fig. 1 Joint detail for EJ-SFC specimen

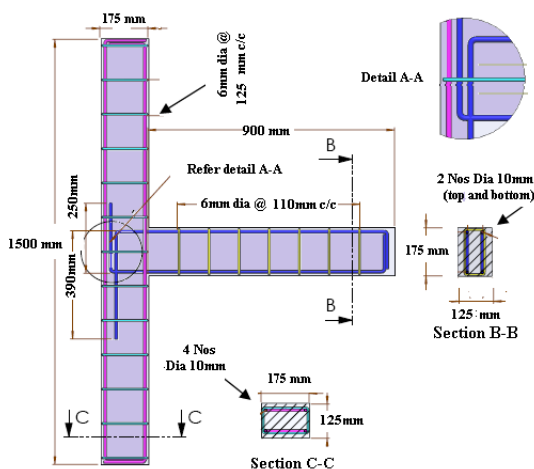


Fig. 2 Joint detail for EJ-IS456 specimen

The uniaxial cracking stress is based upon the characteristic strength of concrete and calculated by $f_{cr} = 0.7 \sqrt{f_{ck}}$. The uniaxial tensile cracking stress is $3.7 \times 10^6 \text{ N/m}^2$ and the uniaxial crushing stress is $38 \times 10^6 \text{ N/m}^2$. The rebar was modelled by using Link 180 element. This element is an isotropic and each two nodes having with three degrees of freedom. For defining the material, the value of EX (Young's modulus) and PRXY (Poisson's ratio) were taken as $2 \times 10^5 \text{ N/mm}^2$ and 0.16 respectively. For modelling the element, EX (Young's modulus) value is $2.1 \times 10^{11} \text{ N/m}^2$ and PRXY (Poisson's ratio) value is 0.3.

B. Modelling

ANSYS 14.5 has been used to model the non-linear finite element analysis. Fig.1 and Fig.2 show the geometrical details of the exterior joint considered for investigation for non-linear finite element analysis. Fig.3 (a) illustrates finite element mesh for all the specimens. Meshing: The accuracy of the results mainly depends on the size of the mesh. The finer mesh gives a very good accurate result than that of coarse mesh. All the concrete elements meshed with size of 25mm and totally 4000 Nos rectangular elements were used. Fig. 3 (a) shows the overall mesh generation for exterior beam-column joint.

C. Material property

Concrete: The designed mix proportion for M20 grade of concrete is 1:2.5:3.33. The cube compressive strength (f_{cu}) under uniaxial compression is determined by the crushing of a standard cube size 150mm. The average cube strength (f_{cu}) after 28 days was 38 N/mm^2 . The cube strength (f_{cu}) and cylindrical strength (f'_c) relationship were $f'_c = 0.8 f_{cu}$. The ultimate compressive strength (f'_c) is 30.4 N/mm^2 . The empirical expression for the static modulus to characteristic cube strength (f_{cu}) is $5000 \sqrt{f_{ck}}$. The relationship between modulus of rupture to the characteristic strength of concrete is (f_{cr}) $= 0.7 \sqrt{f_{cu}}$. The splitting tensile strength is (f_{ct}) $= 2P / \pi DL$. The cylindrical compressive stress (f'_c) is 30.4 N/mm^2 . The flexural tensile strength of the concrete is 4.31 N/mm^2 . The strain in the concrete under direct compression is 0.002 and 0.0035 for flexure. The ultimate shrinkage strain is 0.0003 mm/mm . The co-efficient of thermal expansion of steel is $12 \times 10^{-6} \text{ mm/mm}^\circ\text{C}$ and concrete is $12 \times 10^{-6} \text{ mm/mm}^\circ\text{C}$. The specific weight of the steel is 7850 Kg/m^3 . The uniaxial stress-strain relationship for concrete is $f = E_c / (1 + (\epsilon / \epsilon_0)^2)$, Where $E_c = 2 f'_c / \epsilon_0$. Reinforcement: 10mm bar was used as main bar for both the column and beam and the cross-sectional area of 10mm diameter bar is 80 mm^2 and unit weight per meter was 0.617 kg/m^3 . The yield strength, tensile strength and Elongation were 560 N/mm^2 , 640 N/mm^2 and 15.2% respectively. Similarly, 6mm bar was used as shear reinforcement for both the column and beam. The cross-sectional area of 6mm diameter bar was 29 mm^2 and unit weight per meter was 0.22 kg/m^3 . The yield strength, tensile strength and Elongation were 545 N/mm^2 , 600 N/mm^2 and 16% respectively.

D. Real constants

Material number, volume ratio and orientation angles are the parameters (real constants) to be considered for Solid65 element. All the real constants were set to zero because no smeared reinforcement was used in this model. The diameter of the main reinforcement and shear reinforcement are 10mm and 6mm respectively. Their cross-sectional areas are 78.5 mm^2 and 50.26 mm^2 respectively. The strain and cross sectional area is the real constant for Link 180 element.

E. Loading and boundary condition

For getting a unique solution, displacement boundary conditions are used and this was achieved by providing hinged boundary conditions at both the ends of the column, i.e. zero was entered for the translation at the nodes x, y and z. A constant axial load 40kN was given at column top and this load was maintained till the end of the test and at the end of the beam, reverse cyclic loading was applied. The loading and boundary conditions were same as mentioned above for all the specimens. The test was carried out as per site situation that is column was kept in vertical position and beam was kept in the horizontal position. Fig. 4 (a) illustrates the test setup and hinged boundary condition for exterior joint.

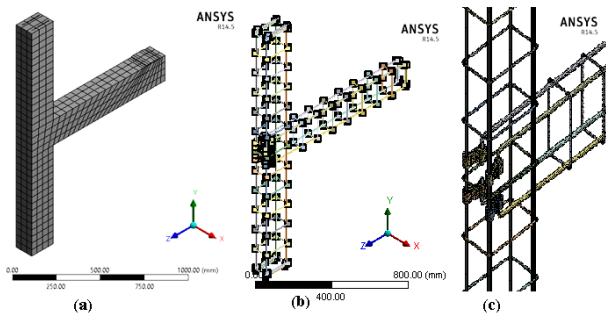


Fig. 3 (a) Typical view of Ansys Model (Concrete) for EJ-SFC specimen
(b) & (c) Typical view of Ansys Model (Reinforcement) for EJ-SFC specimen

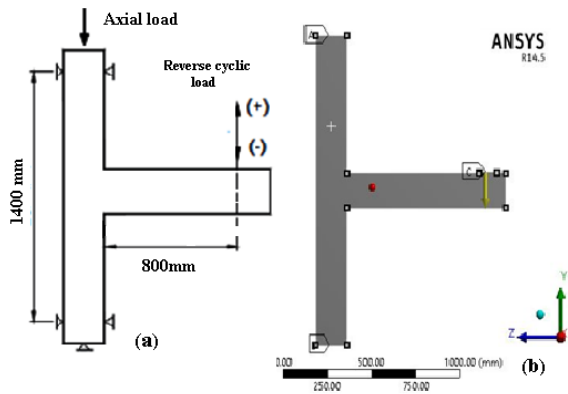


Fig. 4(a) Geometrical Details Of Specimen (B) Load Set Up

V. DISCUSSION OF RESULTS

A. Failure mode of control specimen

The photographic view of the initial crack load and failure mode of the control specimen obtained from the experimental study is illustrated in Fig.5(a) and Fig.5(b). For the control specimen, the first crack was developed at beam front bottom portion at a distance of 50mm from the face of the column. Initially, all the cracks were developed away from the joint and after increasing the load, the cracks were propagated near the neck area of the joint region. The initial flexural cracks were developed at 12mm displacement cycle and diagonal (shear crack) cracks were developed at 35mm displacement cycle. From 2mm displacement cycle to 35mm displacement cycle, all the cracks were only developed in the beam region. The plastic hinge was formed after 42mm displacement cycle and it was only formed at the beam region and not on the core region. The cleavage failure and pull out failure were not developed at the end of the test. This behavior showed that the proposed joint was performed better in reverse cyclic loading condition. The stress distribution obtained from FE analysis of the proposed steel flat coupler joint (EJ-SFC) is illustrated in Fig.6 (a) and Fig.6(b). For the control specimen, the Fig. 6 (a) illustrates the strain contour for downward loading and Fig.6(b) illustrates the strain contour map for upward loading condition. Fig.6(a) and Fig.6(b) indicate the failure mechanism for the control

mechanism for the control specimen.

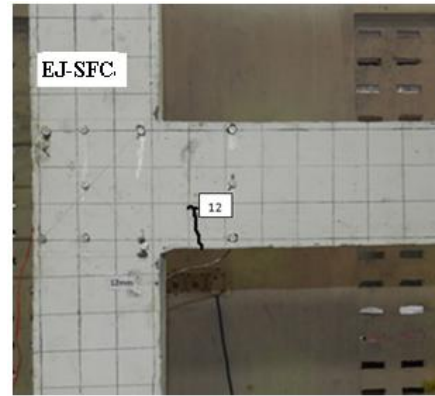


Fig. 5 (a) Crack Pattern At Initial Crack Load For EJ-SFC Specimen

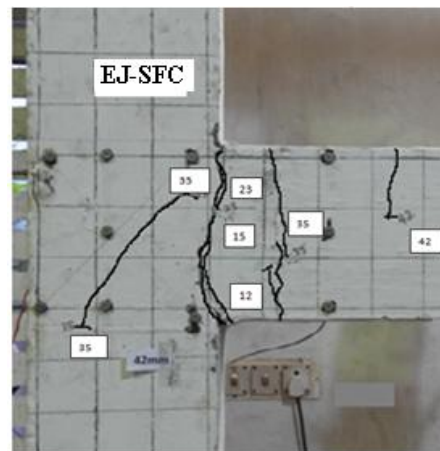


Fig. 5 (b) Photographic View Of Failure Mode For EJ-SFC Specimen

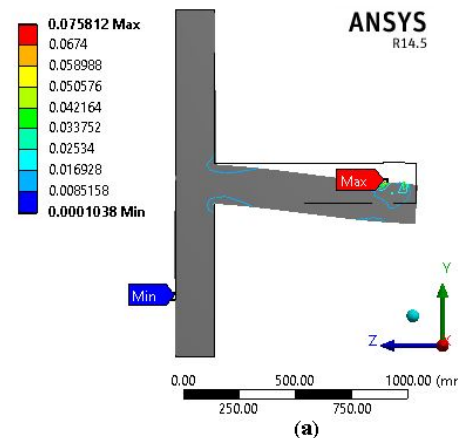


Fig. 6 (a) Strain Contour In Concrete For EJ-SFC Specimen (Push Direction)

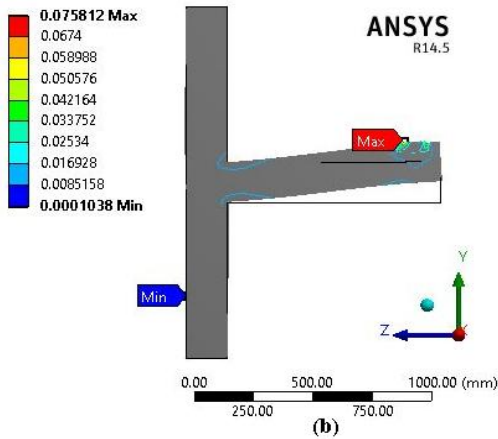


Fig.6 (b) Strain Contour In Concrete For EJ-SFC Specimen (Pull Direction)

B. Failure mode of EJ-IS456 specimen

Fig.7 (a) and Fig.7 (b) show the photographic view of the initial crack load and failure mode of EJ-IS456 specimen obtained from the experimental study. For the EJ-IS456 specimen, the first crack was developed at beam front bottom portion at a distance of 10mm, 20mm and 30mm respectively from the face of the column. Initially, all the cracks were developed in the beam region and after increasing the drift level, the cracks were propagated near the neck area of the beam-column joint region. The initial flexural cracks were developed at 3mm displacement cycle and diagonal (shear crack) cracks were developed at 35mm displacement cycle. At 35mm displacement cycle, many cracks were formed near the neck region. The plastic hinge was formed after 42mm displacement cycle and it was formed at the neck region only and the hinge was slightly penetrated into the core region and no noticeable failures such as cleavage failure and pull out failure were found. The stress distribution obtained from the FE analysis of EJ-IS456 specimen was illustrated in Fig. 8 (a) and Fig. 8 (b) and these figures were indicating the failure mechanism for both the upward and downward loading condition.

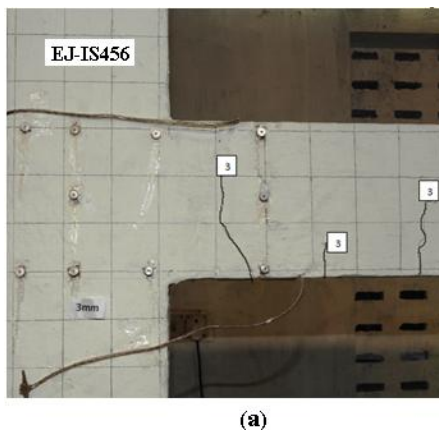


Fig. 7 (a) Initial Crack Formation For EJ-IS456 Specimen

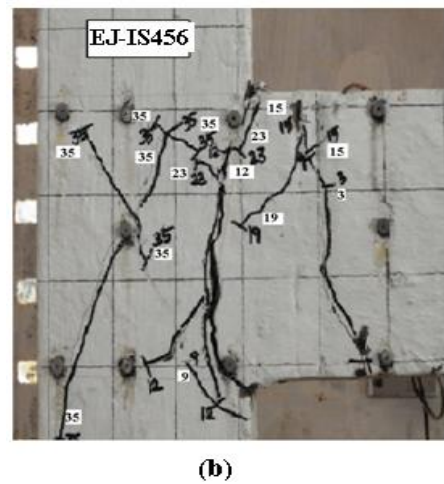


Fig. 7 (b) Final Appearance Of EJ-IS456 Specimen

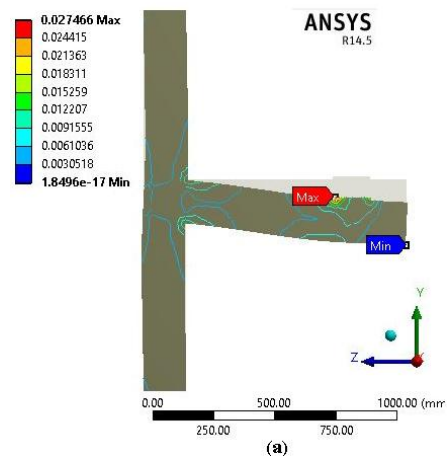


Fig. 8 (a) Strain Contour In Concrete For EJ-IS456 Specimen (Push Direction)

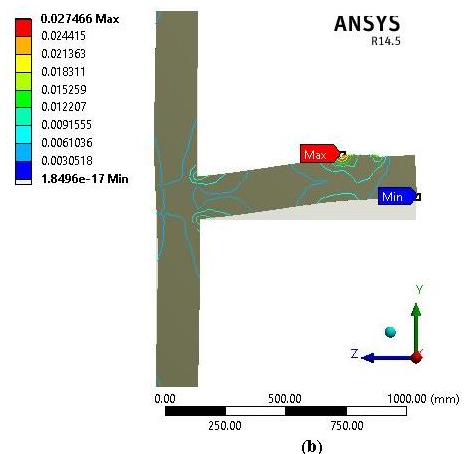


Fig.8 (b) Strain Contour In Concrete For EJ-IS456 Specimen (Pull Direction)

C. Experimental load-deflection plot for control specimen and EJ-IS456 specimen

Fig. 9 shows the load-deflection curve obtained from an experimental study for both the control specimen (EJ-SJC) and EJ-IS456 specimen. The load-deflection curve is clearly indicating the comparative statement for both the downward loading (Push load) and upward loading (Pull load) condition. For the control specimen, the ultimate load was 18.41 kN in pull loading condition and 18.36kN in push loading condition. The average ultimate load for the control specimen is 18.38kN. Similarly, for the EJ-IS456 specimen, the ultimate load determined by the experimental study was 18.41kN in both the pull and push direction. The average ultimate load for EJ-IS456 specimen is 18.41kN. From the above result, it is observed that the load carrying capacity of both the control specimen and EJ-IS456 specimen was same and both the specimens were performed better in terms of ultimate loading condition. From the Fig.9, it is found that the control specimen's ultimate load was remaining same till the end of the test (45mm displacement cycle) which shows the improved ductile behaviour of the proposed specimen (EJ-SFC). But, in the case of EJ-IS456 specimen, the load was decreased from 18.41kN to 14.55kN in positive direction and 15.71kN in negative direction after 35mm displacement cycle. This shows clear indication of the non-ductile behaviour of the EJ-IS456 specimen and the ductility of the specimen was lower than that of the control specimen. Therefore it is concluded that the proposed joint (EJ-SFC) performed well in terms of ductility.

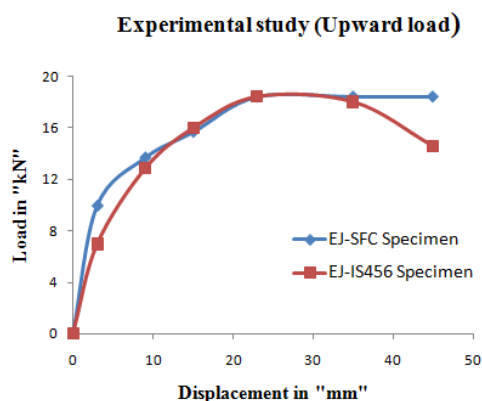


Fig. 9 (a) Load and displacement plot (Upward load) for EJ-SFC and EJ-IS456 (Experimental study)

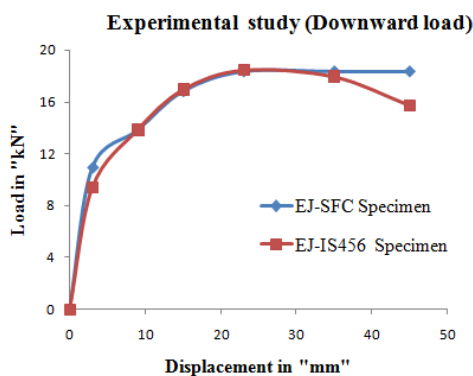


Fig. 9 (b) Load and displacement plot (Downward load) for

EJ-SFC and EJ-IS456 (Experimental study)

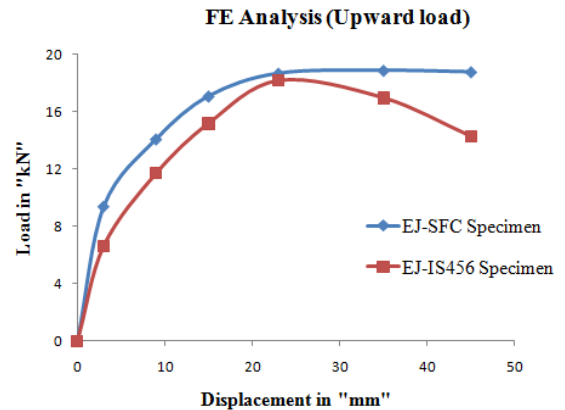


Fig. 10 (a) Load and displacement plot (Upward load) for EJ-SFC and EJ-IS456 (FE analysis)

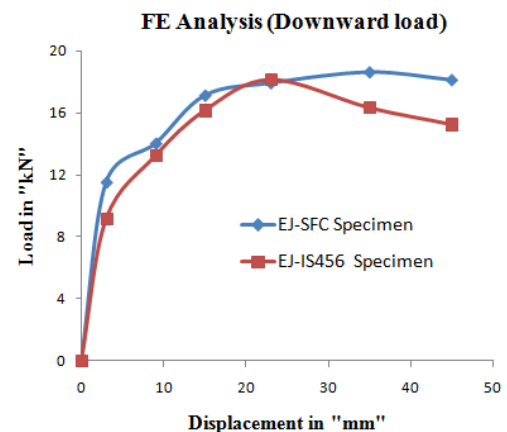


Fig. 10 (b) Load and displacement plot (Downward load) for EJ-SFC and EJ-IS456 (FE analysis)

D. FEA load-deflection plot for control specimen and EJ-IS456 specimen

Fig. 10 shows the load-deflection curve of control specimen and EJ-IS456 which is obtained from numerical study (ANSYS). For the control specimen, the ultimate load was 18.90 kN in pull loading condition and 18.60kN in push loading condition. The average ultimate load for the control specimen is 18.75kN. Similarly, for the EJ-IS456 specimen, the ultimate load determined by the numerical study was 18.21kN in positive direction and 18.12kN in negative direction. The average ultimate load for EJ-IS456 specimen is 18.17 kN. From the above result, it is found that the load carrying capacity of the control specimen is 3% higher than that of EJ-IS456 specimen and it was performed better in terms of resisting the seismic load. From the Fig.10, it is observed that the control specimen's ultimate load was constant till the end of the test (45mm displacement cycle) and no load decrement was found. This behaviour shows the improved ductile behaviour of the control specimen. But, in



the case of EJ-IS456 specimen, the load was decreased from 18.21kN to 14.32kN in positive direction and 18.12kN to 15.23kN in negative direction after 23mm displacement cycle. This shows the non-ductile behaviour of the EJ-IS456 specimen. From the experimental and numerical study (ANSYS), it is concluded that the proposed specimen was superior in terms of ductility and strength.

E. Comparison of experimental and FEA results for EJ-SFC specimen

Fig. 11 shows the ultimate load comparison of EJ-SFC specimen for both upward and downward loading condition. Upward direction: From Fig. 11, it is observed that the behaviour of the specimen was same till 9mm displacement cycle. After that, the load was decreased till 22mm displacement cycle and then the behaviour obtained from both the study was same till the end of the test. Downward direction: The load-deflection behaviour of the EJ-SFC specimen was same in both experimental and numerical analysis.

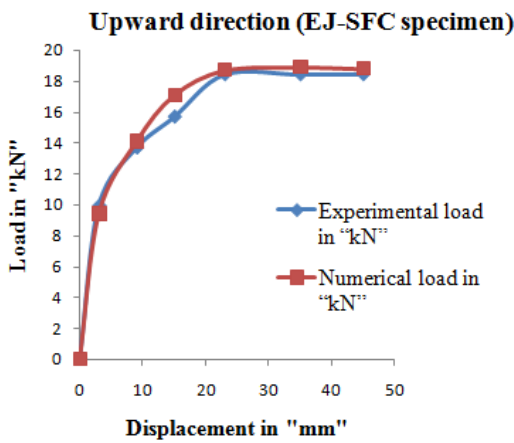


Fig. 11 (a) Load and displacement plot (Upward load) for EJ-SFC specimen

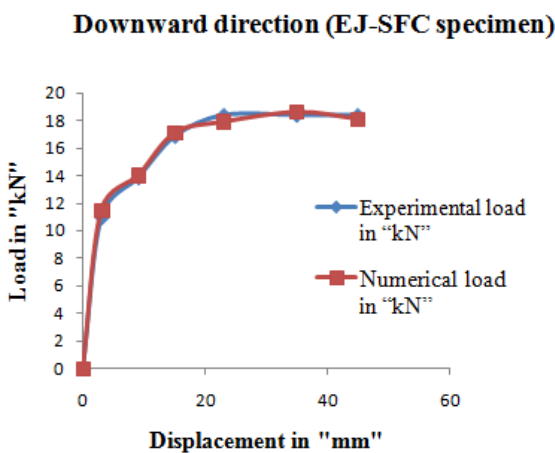


Fig. 11(b) Load and displacement plot(Downward load) for EJ-SFC specimen

Upward load (EJ-IS456 Specimen)

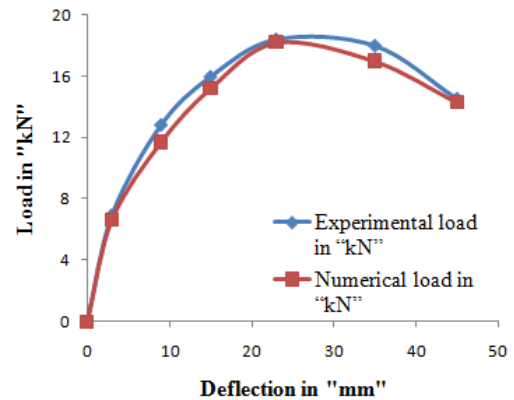


Fig. 12 (a) Load and displacement plot (Upward load) for EJ-IS456 specimen

Downward load (EJ-IS456 Specimen)

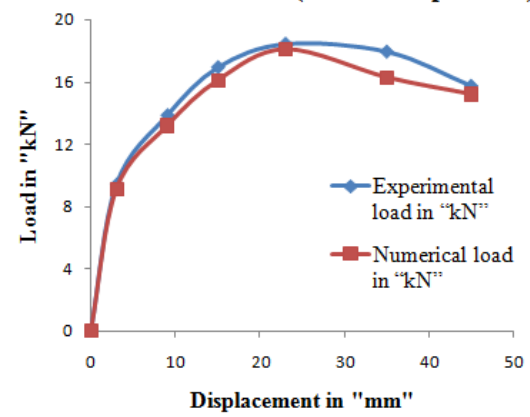


Fig. 12(b) Load and displacement plot (Downward load) for EJ-IS456 specimen

F. Comparison of experimental and FEA results for EJ-IS456 specimen

The load-displacement obtained from both experimental and numerical study is shown in Fig. 12. From the Fig. 12, it is observed that from 9mm displacement cycle to 23mm displacement cycle, there was load increment in experimental values. After this cycle, the behaviour of the specimen was varying and load increment was found in experimental values. This increment in load was continued till the last cycle of the test. For the control specimen (EJ-SFC) and EJ-IS456 specimen, the ultimate load and its corresponding displacement obtained from both experimental and numerical study are presented in Table.1 and Table.2. EJ-SCF specimen: From the Table. 1 and Table.2, it is observed that the ultimate load obtained from the experimental study is 18.41kN in pull loading condition and 18.36kN in push loading condition (refer Fig.13). Similarly, the ultimate load obtained from the numerical study is 18.90kN in pull loading condition and 18.60kN in push loading condition.(refer Fig.13).The range of percentage difference between experimental and numerical load is 1.3 to 2.7%.



EJ-IS456 specimen: From the Table.1 and Table.2, it is observed that the ultimate load obtained from the experimental study is 18.41kN in pull loading condition and 18.40kN in push loading condition (refer Fig.14). Similarly, the ultimate load obtained from the numerical study is 18.21kN in pull loading condition and 18.12kN in push loading condition (refer Fig.14). The range of percentage difference between experimental and numerical load is 1.1 to 1.5%

Table. 1 Ultimate load comparison for EJ-SFC and EJ-IS456 specimen (Positive direction)

Displ ^{*1} . in "mm"	Positive direction		% Diff ^{*3} .
	Exp ^{*2} load in "kN"	Numerical load in "kN"	
Ultimate load for EJ-SFC specimen			
23	18.41	-	2.7
35	-	18.9	
Ultimate load for EJ-IS456 specimen			
23	18.41	-	1.1
35	-	18.21	

*¹-Displacement; *²-Experimental; *³- Percentage difference

Table. 2 Ultimate load comparison for EJ-SFC and EJ-IS456 specimen (Negative direction)

Displ ^{*1} . in "mm"	Negative direction		% Diff ^{*3} .
	Exp ^{*2} . load in "kN"	Numerical load in "kN"	
Ultimate load for EJ-SFC specimen			
23	18.36	-	1.3
35	-	18.6	
Ultimate load for EJ-IS456 specimen			
23	18.40	-	1.5
35	-	18.12	

*¹-Displacement; *²-Experimental; *³- Percentage difference

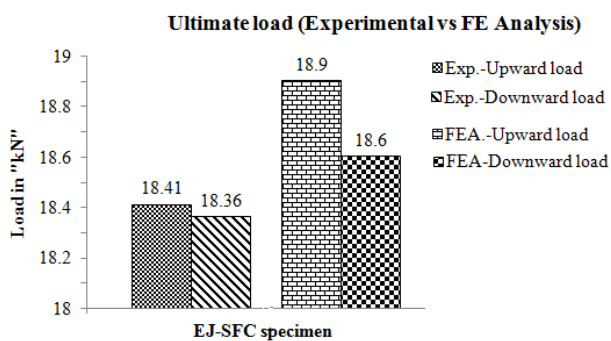


Fig. 13 Ultimate load comparison for EJ-SFC specimen

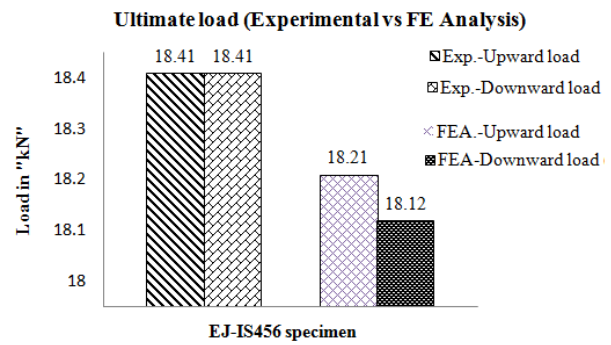


Fig. 14 Ultimate load comparison for EJ-IS456 specimen

VI. CONCLUSIONS

The finite element analysis study was carried out on the exterior joint to assess the use of coupler bar in the joint region. Two groups of half scaled exterior joints were considered for the numerical study. Two different types of anchorage were used for anchoring the beam main bar. In the first group, the beam main bar anchored by coupler bar and the second group of the specimen were anchored by the standard ninety-degree hook as per the requirement of IS456-2000. The entire groups of the specimen were subjected to reverse cyclic loading. The result obtained from the FEA study was compared with the experimental study. Based on the study the following conclusions were drawn:

- The average ultimate load obtained from FEA study of the proposed specimen is 2 % higher than that of experimental study.
- The average ultimate load obtained from FEA study of EJ-IS456 specimen is 3 % higher than that of experimental study.
- The initial crack formation of the proposed specimen was delayed in both the experimental and numerical study.
- The cracks developed in the proposed specimen were minimum than that of EJ-IS456 specimen. In both experimental and numerical study, no pull out failure and no cleavage failure were found in the proposed specimen.
- The ductile behaviour of the proposed specimen is superior and large deformation without a reduction in strength was observed in both experimental and numerical study.
- The load-deflection curve of the proposed specimen and EJ-IS456 was similar and the results obtained from FEA study were very close to experimental results.
- The strain contour obtained from the FE Analysis showed a clear indication of the expected failure location of both the control and EJ-IS456 specimen.

- The study showed that the behaviour of the proposed specimen constructed with steel flat coupler joint is performed well in terms of resisting load and ductility.
- The use of this technique in the joint region may reduce the congestion and reduce the construction difficulties such as fabrication, installation, compaction and casting. Also, this technique can be used for an alternate option for the conventional standard ninety-degree hook.

NOTATION

Displ.	-	Displacement
% Diff.	-	Percentage difference
EJ-SFC	-	Exterior joint with Steel Flat Coupler
EJ-IS456	-	Exterior joint with IS456-2000 detailing
f_{ct}	-	Splitting tensile strength
E_c	-	Young's modulus of concrete
f_{cu}	-	Cube strength
L	-	Height of the cylinder
f_{cu}	-	Cube compressive stress
f_c	-	Cylindrical compressive stress
f_{ck}	-	Characteristic compressive strength of concrete
Fig.	-	Figure
f'_c	-	Cylindrical strength
f_{cr}	-	Uniaxial cracking stress
D	-	Diameter of the cylinder
P	-	Axial load

ACKNOWLEDGEMENT

The authors wish to express their gratitude and sincere appreciation to Technical Education Quality Improvement Programme (TEQUIP) for financing this research work. Also, we would like to extend thanks to Pondicherry Engineering College (PEC), Puducherry, India for purchasing a new equipment and for making it available for the experimental work.

REFERENCE

1. H. R. Ronagh, and H. Baji, (2017), 'On the FE Modeling of FRP-Retrofitted Beam-Column Subassemblies' International Journal of Concrete Structures and Materials, Vol.8, No.2, pp.141-155, June 2014, DOI 10.1007/s40069-013-0047-y, ISSN 1976-0485 / eISSN 2234-1315.
2. Kang T.H.K, (2012), "Prediction of performance of exterior beam-column connection with headed bars subject to load reversal", Engineering Structures, Vol.41, pp.209-217.
3. Karayannis, C.G., (2014), "Mechanics of external RC beam-column joints with rectangular spiral shear reinforcement: experimental verification", Springer, DOI:10.1007/s11012-014-9953-6
4. Kim, J., and LaFave, J. M., (2007) "Key Influence Parameters for the Joint Shear Behavior of Reinforced Concrete (RC) Beam-Column Connections," Engineering Structures, No. 29, pp. 2523-2539, doi: 10.1016/j.engstruc.2006.12.012.
5. Kotsovu, G., and Mouzakis, H., (2011), "Seismic behaviour of RC external joints", "Magazine of Concrete Research, 2011, Volume 63, Issue, 4.
6. Sagbas, G, Vecchio, F.J and Christopoulos, C (2011), "Computational Modelling of Seismic Performance of Beam-Column Subassemblies" Journal of Earthquake Engineering, Volume (15), Issue 4, <https://doi.org/10.1080/13632469.2010.508963>
7. Shaaban, I. G and Said, M, (2018), "Finite element modeling of exterior beam-column joints strengthened by ferrocement under cyclic loading, volume(8),pp. 333-346.

8. Tran, M. T, (2016), "Influence Factors for the Shear Strength of Exterior and Interior Reinforced Concrete Beam-Column Joints" Procedia Engineering 142 (2016) 63 - 70. doi: 10.1016/j.proeng.2016.02.014.
9. Tran, T.M, Pham, T.M and Hadi, M.N.S, (2014), 'A new empirical model for shear strength of reinforced concrete beam-column connections' Magazine of Concrete Research, Volume 66, Issue 10, pp.514-530, <http://dx.doi.org/10.1680/mac.13.00130>.
10. Muhsen, B.A and Umamura, H (2011), New Model for Estimation of Shear Strength of Reinforced Concrete Interior Beam-Column Joints, The Twelfth East Asia-Pacific Conference of Structural Engineering and Construction, Elsevier, Procedia Engineering ,14 (2011), pp.2151-2159, <http://dx.doi:10.1016/j.proeng.2011.07.270>

AUTHORS PROFILE



Dr.S.Kothandaraman is a Professor in Civil Engineering, Pondicherry Engineering College, Puducherry, India. He obtained his BE [1981] in Civil Engineering from Madras University, Chennai, India; ME [1986] in structural Engineering from Bharathiar University, Coimbatore, India; Ph.D [1999] in Civil Engineering from Pondicherry University, Puducherry, India. He is a fellow of Institution of Engineers [India], Life member of Indian Concrete Institute, Life member of Institute for steel Growth and Development and Indian Society for Technical Education. He is the founder Honorary Secretary of Institution of Engineers [India], Puducherry State Center and former Chairman of Indian Concrete Institute, Puducherry centre. His research interest includes Construction Materials and Retrofitting of concrete structures. He has been in this profession for more than three decades. He is nationally well known expert in the field of civil engineering through his scholarly contributions to peer reviewed national and international journals.



Thiru. K.Marimuthu is a Research Scholar pursuing Ph.D in Civil Engineering, Pondicherry Engineering College, Puducherry. He obtained his Diploma in Civil Engineering from Vali Valam Desikar Polytechnic College, Nagapattinam, B.Tech. in Civil Engineering from IRTT-Erode [Bharathiyar University] and M.Tech in Structural Engineering from SASTRA university, Thanjavur. He is life member in Indian Concrete Institute (ICI) and Institution of Engineers (India). He acted as a project engineer for 11 years in execution of various civil construction activities.